Superasymmetric fission of heavy nuclei induced by intermediate-energy protons

A. Deppman,[*] E. Andrade-II,[†] V. Guimarães,[‡] and G. S. Karapetyan[§]
Instituto de Fisica, Universidade de Sao Paulo, P. O. Box 66318, 05315-970 São Paulo, SP, Brazil

O. A. P. Tavares[‖]
Centro Brasileiro de Pesquisas Físicas-CBPF/MCTI Rua Dr. Xavier Sigaud, 150, 22290-180 Rio de Janeiro - RJ, Brazil

A. R. Balabekyan[¶]
Yerevan State University, Faculty of Physics, Alex Manoogian 1, Yerevan 0025, Armenia

N. A. Demekhina[**]
Yerevan Physics Institute, Alikhanyan Brothers 2, Yerevan 0036, Armenia and Joint Institute for Nuclear Research (JINR), Flerov Laboratory of Nuclear Reactions (LNR), Joliot-Curie 6, Dubna 141980, Moscow, Russia

J. Adam[††]
Joint Institute for Nuclear Research (JINR), Flerov Laboratory of Nuclear Reactions (LNR), Joliot-Curie 6, Dubna 141980, Moscow, Russia

F. Garcia[‡‡]
Departamento de Ciências Exatas e Tecnológicas-DCET Centro de PEsquisas em Ciência e Tecnologias das Radiações - CPqCTR Universidade Estadual de Santa Cruz - UESC, Rodovia Jorge Amado km 16, Ilhéus - BA, Brazil

K. Katovsky[§§]
Czech Technical University, Department of Nuclear Reactors, Prague, Czech Republic

(Received 5 September 2013; published 13 December 2013)

In this work we present the results for the investigation of intermediate-mass fragment (IMF) production with the proton-induced reaction at 660 MeV on ^{238}U and ^{237}Np target. The data were obtained with the LNR Phasotron U-400M Cyclotron at Joint Institute for Nuclear Research (JINR), Dubna, Russia. A total of 93 isotopes, in the mass range of $30 < A < 200$, were unambiguously identified with high precision. The fragment production cross sections were obtained by means of the induced-activation method in an off-line analysis. Mass-yield distributions were derived from the data and compared with the results of the simulation code CRISP for multimodal fission. A discussion of the superasymmetric fragment production mechanism is also given.

DOI: 10.1103/PhysRevC.88.064609 PACS number(s): 24.75.+i, 25.85.−w, 25.40.−h, 25.70.−z

I. INTRODUCTION

Nuclear dynamics is a complex problem where puzzling aspects of quantum mechanics and the natural difficulties of many-body systems are interconnected. Besides these factors, the strong interaction, which is not completely understood at present time, adds new challenges for calculations in the nonperturbative regime. Collective nuclear phenomena, such as fission, particle or cluster evaporation, and nuclear fragmentation, offer the possibility to study those complex features of nuclear dynamics. Aside from the interest in fundamental nuclear physics, there are many applications where the knowledge of fragment formation dynamics in nuclear reactions would be helpful. For instance, information on intermediate mass fragment (IMF) cross section is relevant for the design of accelerator-driven systems (ADS) and radioactive ion-beam (RIB) facilities, as well as in the study of resistance of materials to radiation.

Fragments in high energy nuclear collisions can be produced by spallation, fission, and/or multifragmentation processes. Hufner [1], using the mass number of the fragments A and their multiplicity M as classification parameters, defined these processes in the following way:

(1) spallation is the process in which only one heavy fragment with a mass close to the target mass, A_T, is formed (a special case of spallation is the so-called deep spallation where $M = 1$ but $A \sim \frac{2}{3}A_T$);
(2) fission is the process in which $M = 2$ and A is around $A_T/2$;
(3) multifragmentation is the process where $M > 2$ and $A < 50$.

[*]adeppman@gmail.com
[†]esegundo@if.usp.br
[‡]valdir@dfn.if.usp.br
[§]ayvgay@ysu.am
[‖]oaptavares@cbpf.br
[¶]balabekyan@ysu.am
[**]demekhina@nrmail.jinr.ru
[††]iadam@jinr.ru
[‡‡]fermingv@gmail.com
[§§]k.katovsky@sh.cvut.cz

Emission of light particles, with atomic number $Z \leqslant 2$, usually dominates the yield of reaction products for light target nuclei, while for heavy targets spallation and fission residua also give significant contribution. Thus, by adopting the definition that IMF are particles with $A > 4$ but lighter than fission fragments ($A < 100$), they can be formed through the following processes: i) Fission of nuclei mass number in the range of 120–130 [2]; ii) Spallation, including the emission of IMF, the so-called associated spallation [3]; iii) Multifragmentation of heavy nuclei [4].

For heavy targets, multifragmentation would be the only mechanism for the formation of IMF. Indeed, in Ref. [4], it was found that in the inverse-kinematics reaction of $3.65A$ MeV ^{208}Pb on ^{1}H, the formation of ^{12}C nucleus presents the characteristics of multifragmentation, with a possible small contribution of binary process. The formation of IMF was also observed in measurements at lower energies, see Refs. [5–7], but in these cases, the dynamics of the process indicates a binary decay with no evidence for multifragmentation. Hence, the study of the production of IMF by reactions with heavy target nuclei at intermediate energies can give new information on the nuclear dynamics. In the present work, our objective is to present new data on the measured cross sections for residual nuclei in the IMF region, obtained from reactions induced by 660 MeV protons on heavy target nuclei, and the corresponding analysis performed with Monte Carlo calculations using the CRISP code [8,9], as described below.

II. THEORETICAL ASPECTS OF IMF FORMATION

It is generally assumed that, at intermediate energies, the nuclear reaction proceeds in two stages. The first stage would correspond to an incoming fast projectile colliding with a single nucleon or with several nucleons, transferring momentum and energy to the nucleus, and leaving the residual nucleus accompanied by several light particles. The second stage would correspond to the decay of the residual nucleus, which is already in statistical equilibrium, by the emission of nucleons or clusters of nucleons. At high energies, where the excitation energy per nucleon of the residual nucleus is $E_x/A \geqslant 3.5$ MeV/nucleon, multifragmentation of the nucleus can take place. This reaction mechanism differs from evaporation since it describes a sudden breakup of the nucleus instead of a successive emission of particles.

In the framework described above, the formation of IMF from heavy targets at intermediate energies could only be attributed to a process in which fission takes place at some point in a long evaporation chain (both pre- and postfission), which is very unlikely. In fact, the fission probability for heavy nuclei drops very fast as the mass number decreases [10–12], and thus, a long evaporation chain would lead to lower fissility nuclei. Another possibility for the formation of IMF would be a very long evaporation chain leading to light spallation products. This mechanism is limited by the maximum excitation energy allowed for the nucleus before multifragmentation becomes dominant, since evaporation would cool the nucleus before the IMF region is reached. Increasing the excitation energy above the 3.5 MeV/nucleon threshold would only increase the contribution from multifragmentation and, in this way, the IMF formed in reactions with heavy targets should be dominated by fragmentation products. Hence, for excitation energies below the multifragmentation threshold, the formation of IMF from heavy nuclei would be very unlikely.

The formation of IMF was observed in the inverse-kinematics reaction of ^{238}U on proton at $1A$ GeV [5], where the cross sections for 254 light nuclides in the element range of $7 \leqslant Z \leqslant 37$ was measured. Based on a detailed study of the experimental kinematic information, the authors identified such nuclides as binary decay products of a fully equilibrated compound nucleus, whereas clear indications for fast breakup processes were absent. Although these result are corroborated by those from Refs. [6,7], they are in contradiction with the scenario described in Ref. [1]. One possible explanation for the binary production of IMF from reactions induced on heavy targets would be by considering highly asymmetric fission fragments which can still undergo evaporation to form, at the end, a nuclide in the region of IMF. This process would correspond to a modification in the classification given by Hufner [1] by using a less restrictive definition for fission, since in this case, the fragment would have mass number quite different from $A_T/2$. This superasymmetric mechanism would corroborate the conjecture that evaporation and fission are manifestation of a single mechanism, called binary decay [13,14]. A complete investigation of this possibility involves the description of the entire process from the primary interaction of the incident proton up to the evaporation of nucleons from the fission fragments. Such a task can only be performed through the Monte Carlo method.

Here we used the CRISP code to calculate all of the features of the nuclear dynamics during the reaction. CRISP is a Monte Carlo code for simulating nuclear reactions [15] where it is assumed that nuclear reactions can be separated in the two stages already mentioned above: the intranuclear cascade and the evaporation/fission process. This code has been developed during the last 25 years, and it has been successfully used to describe many different reactions. The main characteristic of the intranuclear cascade calculation with CRISP is the multicollisional approach [16,17], where the full nuclear dynamics is considered in each step of the cascade. In this process the nucleus is modeled by an infinite square-potential which determines the level structure for protons and neutrons. The effects of the nuclear potential are present in the transmission of the particles through the nuclear surface or through an effective mass according to the Walecka mean field approximation [18]. The multicollisional calculation is accomplished by constantly updating all of the kinematic variables of all particles inside the nucleus, which opens the possibility for treating more realistically many nuclear phenomena. For instance, the anti-symmetrization criteria, which stipulates a strict observation of the Pauli Principle, allows the separation of the intranuclear cascade from the thermalization process [19]. The effectiveness of such an approach can be verified in the processes which are predominantly dependent on the intranuclear cascade step, such as kaon production and hypernuclei decay. Such

processes have been studied with the CRISP code with results compatible with experiments [20,21]. Also, fission of several nuclei has been studied in the quasi-deuteron region [19], where the Pauli blocking mechanism is very important in the determination of the residual nucleus.

The evaporation/fission competition was first studied with the CRISP code in Refs. [22–24], giving for the first time an explanation for the saturation below the unity for the fissility of heavy nuclei observed in photofission experiments at intermediate energies [25,26]. After, the code was extended to simulate reactions at energies up to 3.5 GeV [27], showing also good agreement with experimental data. After nuclear thermalization, the competition between fission and evaporation processes, which includes neutrons, protons and α particles, is determined by the ratios between their respective widths according to the Weisskopf model for evaporation and to the Bohr-Wheeler model for fission. These ratios are given by

$$\frac{\Gamma_p}{\Gamma_n} = \frac{E_p}{E_n} \exp\{2[(a_p E_p)^{1/2} - (a_n E_n)^{1/2}]\}, \tag{1}$$

and

$$\frac{\Gamma_\alpha}{\Gamma_n} = \frac{2E_\alpha}{E_n} \exp\{2[(a_\alpha E_\alpha)^{1/2} - (a_n E_n)^{1/2}]\}. \tag{2}$$

for evaporation and by

$$\frac{\Gamma_f}{\Gamma_n} = K_f \exp\{2[(a_f E_f)^{1/2} - (a_n E_n)^{1/2}]\}, \tag{3}$$

where

$$K_f = K_0 a_n \frac{[2(a_f E_f)^{1/2} - 1]}{(4A^{2/3} a_f E_n)}, \tag{4}$$

for fission. The parameters a_i stand for the density levels calculated by Dostrovsky's parametrization [28] and E_i is given by

$$\begin{aligned} E_n &= E - B_n, \quad E_p = E - B_p - V_p, \\ E_\alpha &= E - B_\alpha - V_\alpha \quad E_f = E - B_f, \end{aligned} \tag{5}$$

where B_n, B_p, and B_α are the separation energies for neutrons, protons, and α's, respectively, and B_f is the fission barrier. V_i stands for the Coulomb potential.

At each nth step of the evaporation, the excitation energy of the compound nucleus is modified by

$$E^n = E^{n-1} - B - V - \varepsilon, \tag{6}$$

where ε is the kinetic energy of the emitted particle.

If the nucleus undergoes fission, the production of fragments is determined according to the multimodal-random neck rupture model (MM-NRM) [29], which takes into account the collective effects of nuclear deformation during fission by the liquid-drop model and single-particle effects by microscopic shell-model corrections. The microscopic corrections create valleys in the space of elongation and mass number, where each valley corresponds to a different fission mode [29].

According to the MM-NRM, the fragment mass distributions are determined by the uncorrelated sum of the different fission modes. In principle, it is supposed that there are three distinct fission modes for heavy nuclei: symmetric Superlong (S) mode and two asymmetric modes standards I ($S1$) and II ($S2$). In the superlong mode, the fissioning system with mass A_f presents itself at the saddle-point in an extremely deformed shape with a long neck connecting the two forming fragments, which will have masses around $A_f/2$. The standard I mode is characterized by the influence of the spherical neutron shell $N_H \sim 82$ and of the proton shell $Z_H \sim 50$ in the heavy fragments with masses $M_H \sim 132$–134. The standard II mode is characterized by the influence of the deformed neutron shell closure $N = 86$–88 and proton shell $Z_H \sim 52$ in the heavy fragments with masses $M_H \sim 138$–140.

The fission cross section as a function of mass number is then obtained by the sum of three Gaussian functions, corresponding to the three modes mentioned above [30]:

$$\begin{aligned} \sigma(A) = \frac{1}{\sqrt{2\pi}} \Bigg[& \frac{K_{1AS}}{\sigma_{1AS}} \exp\left(-\frac{(A - A_S - D_{1AS})^2}{2\sigma_{1AS}^2}\right) \\ & + \frac{K_{1AS}}{\sigma_{1AS}} \exp\left(-\frac{(A - A_S + D_{1AS})^2}{2\sigma_{1AS}^2}\right) \\ & + \frac{K_{2AS}}{\sigma_{2AS}} \exp\left(-\frac{(A - A_S - D_{2AS})^2}{2\sigma_{2AS}^2}\right) \\ & + \frac{K_{2AS}}{\sigma_{2AS}} \exp\left(-\frac{(A - A_S + D_{2AS})^2}{2\sigma_{2AS}^2}\right) \\ & + \frac{K_S}{\sigma_S} \exp\left(-\frac{(A - A_S)^2}{2\sigma_S^2}\right) \Bigg], \end{aligned} \tag{7}$$

where A_S is the mean mass number determining the center of Gaussian functions; and K_i, σ_i, and D_i are the intensity, dispersion, and position parameters of the ith Gaussian functions. The indexes AS, S designate the asymmetric and symmetric components.

The CRISP code works on an event-by-event basis, and therefore, the parameter A_S in Eq. (1) is completely determined by the mass of the fissioning nucleus A_f, that is, $A_S = A_f/2$. The positions of the heavy and light peaks of the asymmetric components in the mass scale are given by the quantities $A_S + D_{iAS} = A_H$ and $A_S - D_{iAS} = A_L$, where A_H and A_L are the masses of the heavy and light fragment, respectively. The values of $A_H + A_L = 2A_S$ are treated as the mass of the undergoing fission nuclei in the respective channel.

One important observable in the fission process is the charge distribution of a given isobaric chain with mass number A. It is assumed that this charge distribution is well described by a Gaussian function characterized by the most probable charge Z_p of an isobaric chain with mass A (centroid of the Gaussian function) and the associate width parameter Γ_z of the distribution as follows [31,32]:

$$\sigma_{A,Z} = \frac{\sigma_A}{\Gamma_z \pi^{1/2}} \exp\left(-\frac{(Z - Z_p)^2}{\Gamma_z^2}\right), \tag{8}$$

where $\sigma_{A,Z}$ is the independent cross section of the nuclide with charge Z and mass A.

The values for Z_p and Γ_z can be represented as linear functions of the mass number of the fission fragments,

$$Z_p = \mu_1 + \mu_2 A\,, \tag{9}$$

and

$$\Gamma_z = \gamma_1 + \gamma_2 A\,. \tag{10}$$

Here μ_i and γ_i were determined by considering a systematic analysis of atomic number distributions of fission fragments. The values obtained for all parameters used in the present work are reported in Table II.

It is important to emphasize that the CRISP code has been used to simulate nuclear reactions of several kinds, such as those induced by protons [33–35], photons [19,27,36–38], electrons [39,40], or hypernuclei [21,41,42], with energies from 50 MeV up to 3.5 GeV, and on nuclei with masses going from $A = 12$ up to $A = 240$ and with several observables: spallation products, strange particles, fission products, hyperon-decay particles, fragment mass, and atomic number distributions. The code has been applied in the study for development of nuclear reactors [43–45]. Thus, the CRISP code is a reliable tool to investigate properties of nuclear reactions.

III. EXPERIMENTAL PROCEDURE

In the following we describe how the data present in this work have been obtained. A natural uranium target of 0.164 g and 0.0487 mm thick and a neptunium target of 0.742 g and 0.193 mm thick were exposed to an accelerated proton beam of 660 MeV in energy from the LNR Phasotron, Joint Institute for Nuclear Research (JINR), Dubna, Russia [46]. The proton flux was determined by the use of an aluminum monitor with known cross section [47]. The monitor, the same size as the target, was irradiated together with the target. The irradiation time was 27 min and the proton beam intensity was about 3×10^{14} protons per min. The induced activity of the targets was measured by two detectors, an HPGe detector with efficiency of 20% and energy resolution of 1.8 keV (1332 keV ^{60}Co) for the ^{238}U target and a Ge(Li) detector with efficiency of 4.8% and energy resolution of 2.6 keV (1332 keV ^{60}Co) for the ^{237}Np target. The identification of the reaction products and the determination of their production cross section were performed considering the half-lives, energies, and intensities of γ transitions of the radioactive fragments.

In the absence of a parent isotope, the cross section of fragment production for each fragment is determined by using the following equation:

$$\sigma = \frac{\Delta N\ \lambda}{N_p\ N_n\ k\ \epsilon\ \eta\ (1 - \exp(-\lambda t_1))\exp(-\lambda t_2)(1 - \exp(-\lambda t_3))}, \tag{11}$$

where σ denotes the cross section of the reaction fragment production (mb); ΔN is the yield under the photopeak; N_p is the projectile beam intensity (min^{-1}); N_n is the number of target nuclei (in 1/cm^2 units); t_1 is the irradiation time; t_2 is the time of exposure between the end of the irradiation and the beginning of the measurement; t_3 is the time measurement; λ is the decay constant (min^{-1}); η is the intensity of γ transitions; k is the total coefficient of γ-ray absorption in target and detector materials; and ϵ is the γ-ray-detection efficiency.

When the isotope production in the reaction under investigation is direct and independent (I) of the parent nuclei decay, the cross section is determined by Eq. (11). If the yield of a given isotope receives a contribution from the $\beta^{\pm}$ decay of neighboring unstable isobar, the cross section calculation becomes more complicated [48]. If the formation probability of the parent isotope is known from experimental data or if it can be estimated on the basis of other sources, then the independent cross sections of daughter nuclei can be calculated by the relation:

$$\begin{aligned}\sigma_B = {} & \frac{\lambda_B}{(1 - \exp(-\lambda_B t_1))\ \exp(-\lambda_B t_2)(\,1 - \exp(-\lambda_B t_3))} \\ & \times \left[\frac{\Delta N}{N_\gamma\ N_n\ k\ \epsilon\ \eta} - \sigma_A\ f_{AB}\ \frac{\lambda_A\ \lambda_B}{\lambda_B - \lambda_A}\left(\frac{(1 - \exp(-\lambda_A t_1))\ \exp(-\lambda_A t_2)\,(1 - \exp(-\lambda_A t_3))}{\lambda_A^2}\right.\right. \\ & \left.\left. - \frac{(1 - \exp(-\lambda_B t_1))\ \exp(-\lambda_B t_2)\,(1 - \exp(-\lambda_B t_3))}{\lambda_B^2}\right)\right],\end{aligned} \tag{12}$$

where the subscripts A and B in the variables refer to the parent and daughter nucleus, respectively; the coefficient f_{AB} specifies the fraction of nuclei A decaying to nuclei B (this coefficient gives the information on how much the β decay affects our data; and $f_{AB} = 1$ when the contribution from the β decay corresponds to 100%); and ΔN is the total photopeak yield associated with the decays of the daughter and parent isotopes. The effect of the forerunner can be negligible in some limit cases, for example, in the case where the half-life of the parent nucleus is very long, or in the case where the fraction of its contribution is very small. In the case when parent and daughter isotopes could not be separated experimentally, the calculated cross sections are classified as cumulative ones (C).

IV. RESULTS AND DISCUSSION

The mass distribution, as cross sections as a function of mass number A, for the fragment produced by 660 MeV proton induced reactions on uranium and neptunium targets are shown in Figs. 1 and 2. In both distributions a prominent

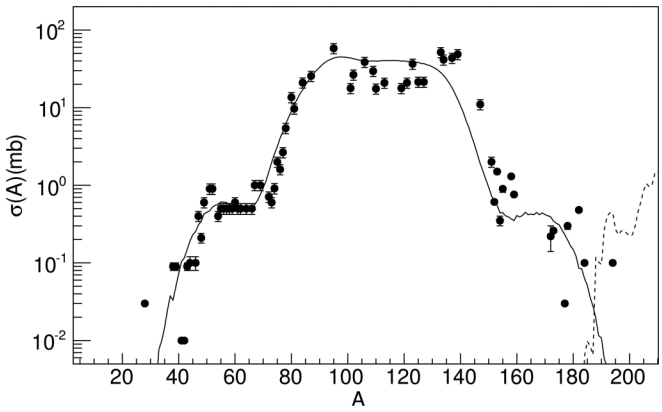

FIG. 1. Mass distribution of binary-decay products from the proton induced reaction at 660 MeV on ^{238}U target. Circles represent the measured isobaric cross sections from the present work and from the data taken from Refs. [46,49,50]. The solid line corresponds to the fission process and the dashed line represents the results of deep-spallation, both calculated with the CRISP code.

peak is observed around the symmetric fragment mass, which is indeed composed of fragments from the symmetric fission mode. The distributions, however, present also a contribution from two asymmetric modes [8,9]. Here we used the code CRISP to interpret these experimental distributions.

Some previous analysis for the mass distributions of the p+^{237}Np and p+^{238}U systems have been performed for the mass range of $70 < A < 150$ [9]. In this work, we have added new data in the region of intermediate mass fragment (IMF) corresponding to $30 < A < 70$ and data in the region of $150 < A < 200$ from Ref. [46]. The measured cross sections for the fragments in the mass range of $30 < A < 70$ are listed in Table I, where the quoted errors include contributions from those associated with the statistical significance of experimental results (2–3%), those in measuring the target thickness (3%), and those in determining the detector efficiency (10%).

Usually, studies on the production of fission fragments do not extend to light nuclei and the inclusion of this region in our analysis can bring up interesting features of the dynamics for fission fragment production. In fact, theoretical calculations, based on the mass asymmetry parameter and fission barrier height [5], have shown that, for heavy targets and for reactions at intermediate or low energies, the cross sections for IMF are very small. As a consequence most of the experimental observations for fission available in the literature seem to die out for atomic numbers below $Z = 28$.

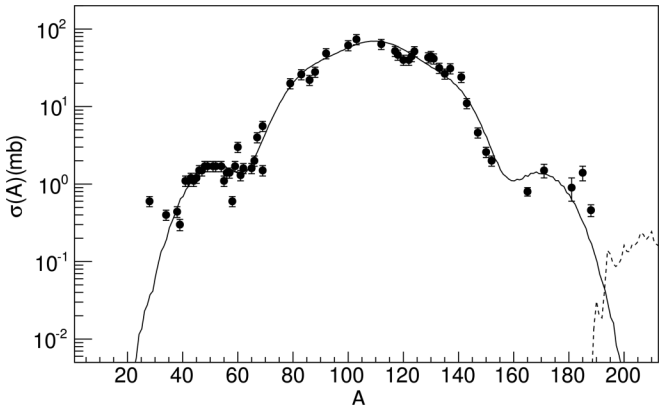

FIG. 2. Idem for the ^{237}Np target.

In Figs. 1 and 2 we can observe a shoulder formed in the mass region of $30 < A < 70$ for both ^{238}U and ^{237}Np target distributions. The presence of IMF in reactions at energy as low as the one of the present study can hardly be attributed to multifragmentation. The observation of another shoulder in the region of $170 < A < 200$, for both distributions, reinforces the idea of a binary process as the origin of the IMF. These observations, therefore, are in agreement with the results obtained by Ricciard *et al.* [5]. In this work, we present the results of a study performed with the simulation code CRISP, where the new experimental data set in the light mass region is described as a possible product of a fission or spallation process. To this end, as described in the next section, we have included an extra superasymmetric fission mode to the code.

V. SUPERASYMMETRIC FISSION MODE

To take into account the possibility of a superasymmetric fission, we included another mode, $S3$, to the CRISP code, which can be described by the usual Gaussian shape from MM-NRM,

$$\sigma(A)_{3AS} = \frac{1}{\sqrt{2\pi}}\left[\frac{K_{3AS}}{\sigma_{3AS}}\exp\left(-\frac{(A - A_S - D_{3AS})^2}{2\sigma_{3AS}^2}\right) + \frac{K_{3AS}}{\sigma_{3AS}}\exp\left(-\frac{(A - A_S + D_{3AS})^2}{2\sigma_{3AS}^2}\right)\right]. \quad (13)$$

As in the case of the three modes previously analyzed in Ref. [9], K_{3AS}, σ_{3AS}, and D_{3AS}, are fitting parameters which allow us to describe the experimental data for fragments produced through the fission channel. In addition to the fission, we calculated the mass distributions for fragments produced by the deep-spallation process. The results are also shown in Figs. 1 and 2, where we observe, that with the inclusion of the superasymmetric mode, the experimental data are well described by the fission mechanism according to the CRISP calculations. The deep-spallation mechanism gives only a very small contribution in the region of heavy fragments, showing that, in fact, the superasymmetric fission is the relevant mechanism for the production of fragments in the region of $160 < A < 200$.

The best-fit values for the parameters used in the MM-NRM approach are shown in Table II. The parameters for the S, $S1$, and $S2$ modes were already discussed in Ref. [9]. Therefore, we focus here on the parameters for $S3$. The superasymmetric mode contributes with 0.6% and 1.2% of the total fission cross section for the ^{238}U and for ^{237}Np targets, respectively. The total fission cross sections are 1140 mb for ^{238}U and 1360 mb for ^{237}Np. The width for the $S3$ distribution is somewhat larger than those for $S1$ and $S2$, but smaller than that for S mode. The most striking feature of the superasymmetric mode is the mass number gap around 60 a.m.u. with respect

TABLE I. Cross section for the measured IMFs products from reaction induced by 660 MeV protons on ^{238}U and ^{237}Np targets.

Element	Type	Cross section, mb		Element	Type	Cross section, mb	
		^{238}U	^{237}Np			^{238}U	^{237}Np
^{28}Mg	C	$0.0043 \pm 4.3\times10^{-4}$	0.186 ± 0.020	^{52}Fe	I	$6.5\times10^{-4} \pm 5.5\times10^{-5}$	0.01 ± 0.01
^{34}Cl^{m}	C	$7.7\times10^{-4} \pm 1.5\times10^{-5}$	0.08 ± 0.02	^{54}Mn	I	0.11 ± 0.01	0.28 ± 0.03
^{38}S	I	$0.007 \pm 1.4\times10^{-4}$	$\leqslant 0.08$	^{55}Co	C	0.02 ± 0.002	$\leqslant 0.036$
^{38}Cl	I	0.04 ± 0.008	$\leqslant 0.28$	^{56}Mn	C	0.15 ± 0.02	0.69 ± 0.07
^{39}Cl	C	0.053 ± 0.005	0.023 ± 0.003	^{56}Co	I	0.07 ± 0.01	0.03 ± 0.006
^{41}Ar	C	$0.0037 \pm 7.4\times10^{-4}$	0.73 ± 0.07	^{56}Ni	I	$\leqslant 0.002$	$\leqslant 0.007$
^{42}K	C	$0.007 \pm 7.0\times10^{-4}$	$\leqslant 0.40$	^{57}Co	I	0.059 ± 0.006	0.20 ± 0.02
^{43}K	C	0.023 ± 0.002	0.45 ± 0.06	^{57}Ni	C	$0.0011 \pm 1.1\times10^{-4}$	$\leqslant 0.01$
^{43}Sc	C	0.012 ± 0.001	0.23 ± 0.02	^{58}Co^{m+g}	I	0.17 ± 0.02	0.13 ± 0.02
^{44}Ar	C	$\leqslant 2.5\times10^{-4}$	0.089 ± 0.02	^{59}Fe	C	0.27 ± 0.03	1.21 ± 0.12
^{44}K	I	$0.031 \pm 5.0\times10^{-5}$	0.22 ± 0.04	^{60}Co^{m+g}	C	0.33 ± 0.03	1.70 ± 0.20
^{44}Sc^{g}	I	$\leqslant 0.0025$	$\leqslant 0.15$	^{60}Cu	C	$\leqslant 0.006$	$\leqslant 0.053$
^{44}Sc^{m}	I	0.065 ± 0.007	0.12 ± 0.01	^{61}Cu	C	0.04 ± 0.004	$\leqslant 0.057$
^{45}K	C	–	0.24 ± 0.05	^{65}Ni	C	$0.0017 \pm 1.7\times10^{-4}$	$\leqslant 0.04$
^{46}Sc^{m+g}	I	0.036 ± 0.004	0.94 ± 0.09	^{65}Zn	I	0.10 ± 0.01	0.87 ± 0.17
^{47}Ca	C	0.024 ± 0.002	$\leqslant 0.067$	^{65}Ga	C	$\leqslant 0.02$	$\leqslant 0.043$
^{47}Sc	I	0.17 ± 0.02	0.63 ± 0.06	^{66}Ni	C	0.015 ± 0.002	0.20 ± 0.05
^{48}Sc	I	0.044 ± 0.004	0.42 ± 0.04	^{66}Ga	I	0.051 ± 0.005	$\leqslant 0.084$
^{48}V	I	0.022 ± 0.002	0.48 ± 0.05	^{66}Ge	C	$\leqslant 0.003$	$\leqslant 0.13$
^{48}Cr	I	$\leqslant 0.0014$	0.01 ± 0.001	^{67}Cu	C	0.55 ± 0.06	2.10 ± 0.21
^{49}Cr	C	0.025 ± 0.005	0.073 ± 0.015	^{67}Ga	C	0.06 ± 0.006	0.20 ± 0.02
^{51}Cr	C	0.41 ± 0.04	0.20 ± 0.02	^{69}Zn^{m}	C	0.041 ± 0.004	0.80 ± 0.16
^{52}Mn^{g}	I	$0.0015 \pm 1.5\times10^{-4}$	0.077 ± 0.008	^{69}Ge	C	0.03 ± 0.003	0.051 ± 0.012
^{52}Mn^{m}	I	$0.0085 \pm 8.5\times10^{-4}$	0.205 ± 0.03				

to the symmetric fragment for both cases studied here. Our results confirm that IMF at intermediate energies are formed predominantly through a binary process, and that it is described by a superasymmetric fission mode.

As shown in the present work, a good description of the fragment production for the full range of mass of $30 < A < 200$ was obtained by considering the fission mechanism. This might indicate that this is, in fact, the actual predominant mechanism. However, we can not totally exclude the possibility that a description of the experimental data would also be achieved by considering some other sort of mechanism, such as evaporation with the inclusion of the associated spallation and with emission of fragments heavier than the α particle.

TABLE II. Parameters for the mass distribution calculations.

Parameter	^{238}U	^{237}Np
K_{1AS}	$(2.0 \pm 5.0)\%$	$(1 \pm 1)\%$
σ_{1AS}	3.5 ± 0.8	4.5 ± 0.4
D_{1AS}	18.5 ± 0.4	21.3 ± 0.4
K_{2AS}	$(19 \pm 5)\%$	$(7.7 \pm 0.8)\%$
σ_{2AS}	6.0 ± 0.5	6.5 ± 0.6
D_{2AS}	18.0 ± 0.4	28.3 ± 0.5
K_{3AS}	$(0.5 \pm 0.5)\%$	$(1.2 \pm 0.3)\%$
σ_{3AS}	7.0 ± 0.5	8.0 ± 0.7
D_{3AS}	57.0 ± 0.4	62.0 ± 0.3
K_S	$(56 \pm 5)\%$	$(79.0 \pm 7.0)\%$
σ_S	13.0 ± 0.5	13.7 ± 1.0
μ_1	4.1 ± 0.6	5.0 ± 0.8
μ_2	0.38 ± 0.01	0.37 ± 0.01
γ_1	0.92 ± 0.08	0.59 ± 0.02
γ_2	0.003 ± 0.001	0.005 ± 0.0002

VI. CONCLUSION

The cross sections for fragments produced by the proton-induced fission on ^{238}U and ^{237}Np at 660 MeV were measured at the LNR Phasatron (JINR). The fragment mass distributions covering the region of $20 < A < 200$, allowed the investigation of the production mechanism for the intermediate mass fragments (IMF) in the mass range of $20 < A < 70$. It was found that, for each of the IMF observed in the low mass region, there was a heavier counterpart in the region of $170 < A < 200$, indicating that they are actually produced by a binary process. This hypothesis was tested with the use of the CRISP code by including an additional superasymmetric fission mode described according to the MM-NRM approach. The results show, indeed, that it is possible to give an accurate description of the fragment production in the entire mass region of $20 < A < 200$ by considering the evaporation/fission mechanism in the CRISP code with the usual

fission modes, namely, one symmetric and two asymmetric, and including a fourth superasymmetric mode. This last mode produces fragments that are around 60 a.m.u., far from the symmetric fragment mass, and contributes with 0.6% and 1.2% to the total fission cross section for ^{238}U and ^{237}Np, respectively. Our results are in agreement with previous results obtained by Ricciardi *et al*. [5] evidencing the binary production mechanism for the IMF at intermediate energy nuclear reaction.

ACKNOWLEDGMENTS

G.K. is grateful to the Fundação de Amparo à Pesquisa do Estado de São Paulo (FAPESP) 2011/00314-0 and 2013/01754-9, and also to the International Centre for Theoretical Physics (ICTP) under the Associate Grant Scheme. A.D. acknowledges the partial support from CNPq under grant no. 305639/2010-2 and FAPESP under Grant No. 2010/16641-7. E.A. acknowledges the support from FAPESP under Grant No. 2012/13337-0. We thank Prof. Wayne Seale for reviewing the text.

[1] J. Hufner, Phys. Rep. **125**, 129 (1985).
[2] W. Loveland, C. Luo, P. L. McGaughey, D. J. Morrissey, and G. T. Seaborg, Phys. Rev. C **24**, 464 (1981).
[3] Y. Yariv and Z. Fraenkel, Phys. Rev. C **20**, 2227 (1979).
[4] B. Grabez, Phys. Rev. C **48**, R2144 (1993).
[5] M. V. Ricciardi, P. Armbruster, J. Benlliure *et al*., Phys. Rev. C **73**, 014607 (2006).
[6] A. A. Kotov, L. N. Andronenko, M. N. Andronenko *et al*., Nucl. Phys. A **583**, 575 (1995).
[7] H. W. Barz, J. P. Bondorf, H. Schulz *et al*., Nucl. Phys. A **460**, 714 (1986).
[8] A. Deppman, E. Andrade-II, V. Guimarães, G. S. Karapetyan, and N. A. Demekhina, Phys. Rev. C **87**, 054604 (2013).
[9] A. Deppman, E. Andrade-II, V. Guimarães, G. S. Karapetyan, A. R. Balabekyan, and N. A. Demekhina, Phys. Rev. C **88**, 024608 (2013).
[10] D. A. de Lima, J. B. Martins, and O. A. P. Tavares, Il Nuovo Cim. A **103**, 701 (1990).
[11] M. L. Terranova and O. A. P. Tavares, Phys. Scr. **49**, 267 (1994).
[12] T. Fukahori, O. Iwamoto, and S. Chiba, in *Proceedings of the 7th International Conference on Nuclear Criticality Safety, ICNC 2003*, JAERI-conf, 2003-019, edited by Nihon Genshiryoku Kenkyuujo and Nihon Genshiryoku Gakkai (Japan Atomic Energy Research Institute, Tokai-mura, Japan, 2003), Parts 1–2, p. 144.
[13] L. G. Moretto, Nucl. Phys. A **247**, 211 (1975).
[14] S. B. Duarte, O. A. P. Tavares, F. Guzman *et al*., Atom. Data and Nucl. Data Tables **80**, 235 (2002).
[15] A. Deppman, S. B. Duarte, G. Silva *et al*., J. Phys. G: Nucl. Part. Phys. **30**, 1991 (2004).
[16] T. Kodama, S. B. Duarte, K. C. Chung, and R. A. M. S. Nazareth Phys. Rev. Lett. **49**, 536 (1982).
[17] M. Goncalves, S. de Pina, D. A. Lima *et al*., Phys. Lett. B **406**, 1 (1997).
[18] B. D. Serot and J. D. Walecka, in *Advances in Nuclear Physics* edited by J. W. Negele and E. Vogt, Vol. 16 (Plenum Press, New York, USA, 1986), p. 1.
[19] A. Deppman *et al*., J. Phys. G: Nucl. Part. Phys. **30**, 1991 (2004).
[20] S. de Pina *et al*., Phys. Lett. B **434**, 1 (1998).
[21] I. Gonzalez *et al*., J. Phys. G: Nucl. Part. Phys. **38**, 115105 (2011).
[22] A. Deppman *et al*., Phys. Rev. Lett. **87**, 182701 (2001).
[23] A. Deppman *et al*., Nucl. Instrum. Methods Phys. Res. B **211**, 15 (2003).
[24] A. Deppman *et al*., Comp. Phys. Comm. **145**, 385 (2002).
[25] N. Bianchi *et al*., Phys. Lett. B **299**, 219 (1993).
[26] J. C. Sanabria *et al*., Phys. Rev. C **61**, 034604 (2000).
[27] A. Deppman, G. Silva, S. Anefalos, S. B. Duarte, F. García, F. H. Hisamoto, and O. A. P. Tavares, Phys. Rev. C **73**, 064607 (2006).
[28] I. Dostrovsky, P. Rabinowitz, and R. Bivins, Phys. Rev. **111**, 1659 (1958).
[29] U. Brosa, S. Grossman, and A. Muller, Z. Naturforschung **41**, 1341 (1986).
[30] W. Younes, J. A. Becker, L. A. Bernstein *et al*., *Nuclear Physics in the 21st Century: International Nuclear Physics Conference (INPC 2001)* (AIP, New York, 2001) [AIP Conf. Proc. **610**, 673 (2001)].
[31] H. Kudo, M. Maruyama, M. Tanikawa, T. Shinozuka, and M. Fujioka, Phys. Rev. C **57**, 178 (1998).
[32] M. C. Duijvestijn, A. J. Koning, J. P. M. Beijers, A. Ferrari, M. Gastal, J. van Klinken, and R. W. Ostendorf, Phys. Rev. C **59**, 776 (1999).
[33] S. A. Pereira *et al*., Nucl. Sci. Eng. **159**, 102 (2008).
[34] E. Andrade-II *et al*., J. Phys. G: Nucl. Part. Phys. **38**, 085104 (2011).
[35] E. Andrade-II, J. C. M. Menezes, S. B. Duarte *et al*., EPJ Web Conf. **21**, 10001 (2012).
[36] A. Deppman, O. A. P. Tavares, S. B. Duarte, J. D. T. Arruda-Neto, M. Gonçalves, V. P. Likhachev, and E. C. de Oliveira, Phys. Rev. C **66**, 067601 (2002).
[37] E. Andrade-II, E. Freitas, O. A. P. Tavares *et al*., *XXXI Workshop on Nuclear Physics in Brazil* (AIP, New York, 2009) [AIP Conf. Proc. **1139**, 64 (2009)].
[38] A. Deppman, G. Silva, S. Anefalos, S. B. Duarte, F. García, F. H. Hisamoto, and O. A. P. Tavares, Phys. Rev. C **73**, 064607 (2006).
[39] V. P. Likhachev *et al*., Nucl. Phys. **713**, 24 (2003).
[40] V. P. Likhachev *et al*., Phys. Rev. C **68**, 014615 (2003).
[41] I. Gonzales *et al*., J. Phys. Conf. Series **312**, 022017 (2011).
[42] F. Krmpotic *et al*., *Nuclear Structure and Dynamics 2012* (AIP, New York, 2012) [AIP Conf. Proc. **1491**, 117 (2012)].
[43] S. Anefalos *et al*., *International Conference on Nuclear Data for Science and Technology 2004* (AIP, New York, 2004) [AIP Conf. Proc. **769**, 1299 (2005)].
[44] S. Anefalos *et al*., Nucl. Sci. Eng. **151**, 82 (2005).
[45] A. Deppman *et al*., Sci. Tech. Nucl. Inst. **2012**, 480343 (2012).
[46] J. Adam, K. Katovsky, R. Michel, and A. Balabekyan, *International Conference on Nuclear Data for Science and Technology 2004* (AIP, New York, 2004) [AIP Conf. Proc. **769**, 1043 (2005)].
[47] J. B. Cumming, Ann. Rev. Nucl. Sci. **13**, 261 (1963).
[48] H. Baba, J. Sanada, H. Araki *et al*., Nucl. Instrum. Methods Phys. Res. A **416**, 301 (1998).
[49] G. S. Karapetyan, A. R. Balabekyan, N. A. Demekhina, and J. Adam, Phys. At. Nucl. **72**, 911 (2009).
[50] A. R. Balabekyan, G. S. Karapetyan, N. A. Demekhina *et al*., Phys. At. Nucl. **73**, 1814 (2010).